High-Bandwidth Power Hardware-in-the-Loop for Motor and Battery Emulation at High Voltage Levels

Manuel Fischer, Philipp Kemper, Johannes Herbold, Daniel Epping, Frank Puschmann
dSPACE GmbH
Real-Time Test & Development Solutions
Paderborn, Germany
Tel.: +49 5251 1638-0
E-Mail: MaFischer@dspace.de
ORCiD: 0000-0002-5499-697X
URL: http://www.dspace.com

Keywords

«Power Hardware-in-the-Loop», «Machine emulation», «Modular converter», «Interleaved converters», «Test bench».

Abstract

Power hardware-in-the-loop (PHIL) emulation of batteries and electric machines is an efficient method to accelerate the development and testing process of traction inverters and their control systems at different operating conditions. This paper presents the overall setup of a high-bandwidth, high-voltage PHIL system. Real-time machine and battery models, a control unit for the power electronics device and the power electronic device itself are highlighted as the most relevant parts of the PHIL system. Multiple approaches fulfilling the requirements of these parts are explained in detail. Finally, this paper determines the most suitable approaches to setting up a modular PHIL system that is scalable in terms of power range and number of output connectors.
The overall hardware of the PHIL system with the described components is set up. Concluding measurement results prove its performance.

Introduction

Electromobility is one of the mega trends in the automotive industry. The drivetrain of an electrically powered car generally consists of a high-voltage (HV) battery, a traction inverter and an electric machine. Throughout the development process, testing plays a decisive role. In addition to proving the entire system's functionality, reliability and safety, testing can also improve efficiency by enhancing the control. These hardware tests must proceed in conformance with common standards, such as ISO 26262, ISO 21498 and ISO 21782.
Typically, a dynamometer test bench is set up for this purpose, see Fig. 1. The investigated machine is coupled to a load machine in order to set several mechanical operating points. The device under test (DUT) inverter converts the battery's DC voltage to the required voltage courses feeding all the phases of the investigated machine. These dynamometer test benches are expensive and challenging to set up. Moreover, they cannot flexibly used for different machine settings or battery behavior. Alternatively, the DUT inverter can be tested by using power hardware-in-the-loop (PHIL) simulators. For this, the DUT inverter's input and output terminals are connected to a power electronics device which has the same electrical characteristic as the investigated battery and machine, see Fig. 1.
The PHIL test bench consists of three main components:

- A battery and a machine model, which calculate the investigated battery's and machine's electrical behavior in real-time depending on the DUT inverter's switching behavior,
- A control unit, which controls the power electronic devices in a way that the same load currents occur as in the real-world dynamometer test bench,
- The power electronics devices itself, which adjust the desired load currents.

The use of a common switched-mode operated power electronics device in PHIL application leads to additional disturbing ripple content in the output current which differs from the reference current. The following concepts have already been investigated and offer a solution that minimizes the additional ripple content. Generally, a setup using a multi-branch inverter with an interleaved modulation technique [1-5] is recommended. This topology leads to an increasing effective switching frequency at the output terminals and thereby decreases the additional ripple content. Adding a passive LC filter at the output terminals of a switched-mode operated two-level or multi-level inverter decreases the additional ripple as well, but has to work with a lower bandwidth of the output voltage [6-12]. In [13,14] a linear amplifier is suggested, albeit only for medium and low voltage levels. Specialized concepts are a four-level inverter with variable output voltages and a modular multilevel converter [15-17].
This paper presents the setup of an entire PHIL system. A modular concept is used for the power electronics devices emulating the battery and the investigated machine. These power electronics modules are based on multilevel half bridge branches connected in parallel which fulfill the requirements for high voltage, high bandwidth as well as a small additional emulator current ripple. Moreover, two different control schemes – voltage-based and current-based – are presented and implemented on the control unit. The theory of the machine and the battery model as well as measurement results of the PHIL system complete this work.

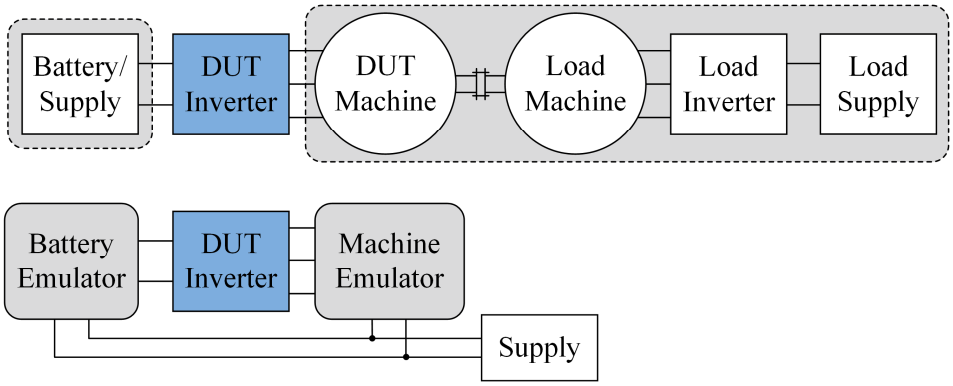

Fig. 1: Schematic diagram of a common dynamometer test bench (top) compared to a PHIL test bench (bottom)

Overview of the PHIL System

Fig. 2 depicts a schematic diagram of the entire PHIL system. The DUT inverter is connected to the common DC link $V_{DC,Sup}$ via power electronics (PE) modules. The PE modules at the DUT inverter's DC terminals emulate the behavior of the battery. By measuring the input currents i_{Bat+} and i_{Bat-} the battery model can evaluate the actual state and especially the output voltage $v_{Bat,ref}$ of the emulated battery. This reference output voltage is passed to the device control unit which determines the switching commands SC for the dedicated PE modules on the battery side. The PE modules at the three DUT inverter's AC terminals emulate the behavior of the investigated machine. By measuring the output voltages $v_{DUT,x}$ (with x = U,V,W), the machine model can calculate the actual state of the emulated machine and thereby especially the machine's input currents $i_{M,ref,x}$. In addition, the emulator outputs all relevant interfaces, for example, communication or position sensor emulation. The reference currents are passed to the device control unit which determines the switching commands SC for the PE modules on the machine side. When the virtual machine is in motor mode, the battery PE modules feed the DUT inverter and the machine PE modules feed the inverter's output power back into the common DC link (and vice versa when the virtual machine is in generative mode). Consequently, the power flow circulates and the supply unit feeds only the power losses of the system. In this case, no bidirectional grid connection or galvanically isolated DC/DC converters are required. In the following sections, the relevant parts of the PHIL system are explained in detail.

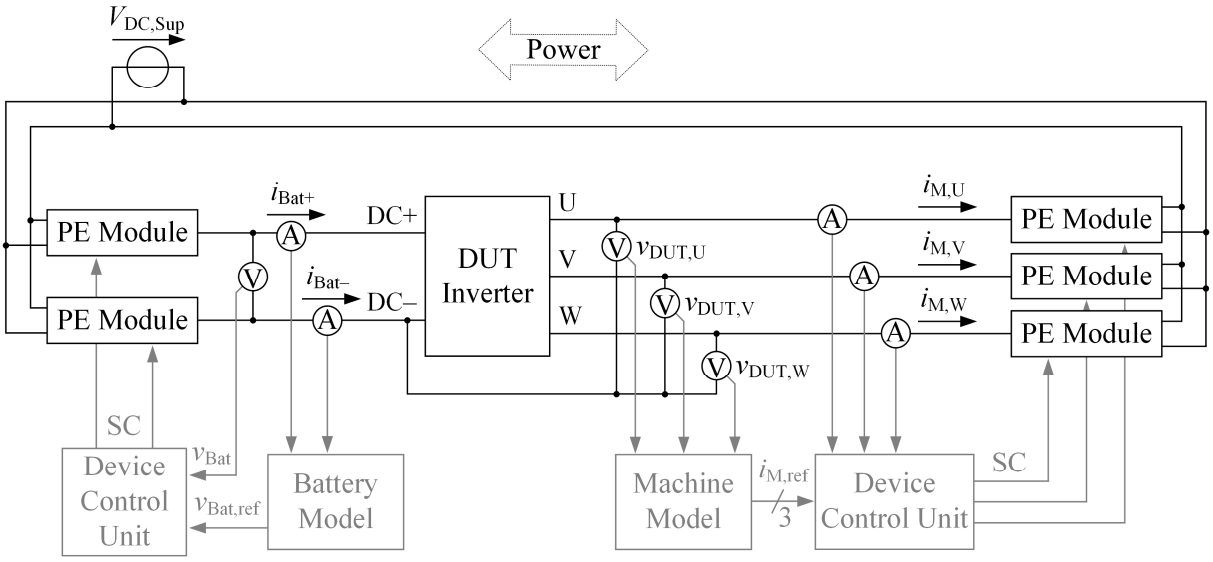

Fig. 2: General overview diagram of the entire PHIL system

Power Electronics Modules

In a PHIL application, the PE modules have to overcome multiple challenges: the HV level with DC voltages above 1,000 V, the demand for a high output current with a bandwidth of a few kHz, the capability for allowing bidirectional power flow, insertion of additional current ripple that has to be as low as possible, and modularity so it can operate multiple modules in parallel. Moreover, the electronic loads must be able to fulfill any conceivable electrical operation point. Therefore, systems with any kind of derating functions, like power hyperbola, do not meet the motor emulation demands.

A topology which fulfills these requirements is a multi-branch three-level NPC inverter, see Fig. 3. Additional output voltage levels compared to a conventional two-level inverter decrease the currents' total harmonic distortion. Moreover, in every switching state the DC link voltage $V_{DC,Sup}$ drops over at least two switches. Hence, each switch only has to feature an electric strength of half the DC link voltage. The switches are executed as fast-switching silicon-carbide MOSFETs. On each module, three NPC half bridge branches are connected in parallel. Consequently, the output current can be three times higher than the maximum current of a single branch. The three branches are each coupled in pairs by three differential-mode chokes. If the current is symmetrically distributed between the three branches, the magnetic flux inside the differential-mode chokes will be nearly zero and only the choke's magnetic leakage flux will be effective. Otherwise, in case of asymmetric distribution, the occurring magnetic flux leads to an inductance, which counteracts the asymmetry. Consequently, depending on the

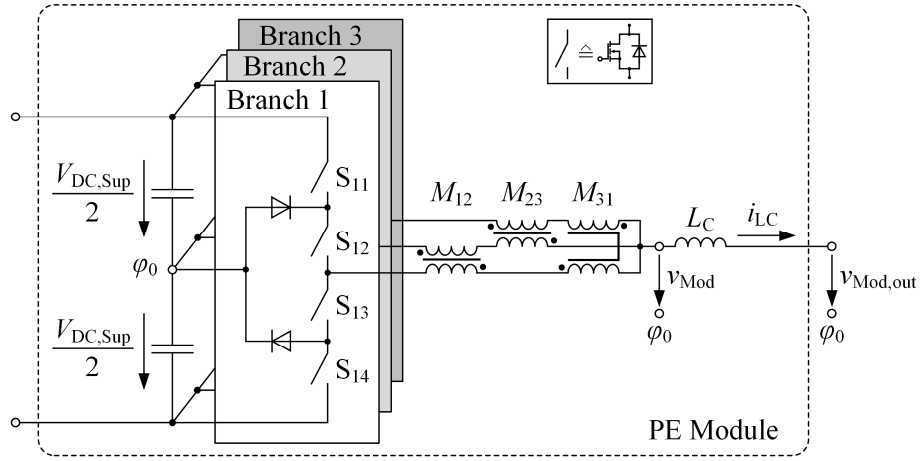

Fig. 3: Schematic of an implemented PE module

switching states of the three branches, the output voltage v_{Mod} at the common coupling point can assume seven discrete voltage states:

$$v_{Mod} = \pm \frac{k}{6} \cdot v_{DC,Sup} \qquad \text{with } k = \{0, 1, 2, 3\} \tag{1}$$

After the coupling point, a further coupling inductance L_C is connected in series, which acts as controlled system between the DUT inverter and the PE modules.

Machine and Battery Model

The accuracy of the machine and battery models defines the quality of the emulation results. Nevertheless, one basic requirement has to be fulfilled: Both models have to run in real-time. In this paper, a three-phase, permanent magnet synchronous machine is emulated. Possible real-time models are a common or an extended fundamental component model [18,19], a magnetic equivalent circuit (MEC) model [20] or a simplified analytical model [21]. All of them use the machine's terminal voltages as input variables and calculate the three load currents. An efficient way to simulate nonlinearities, e.g., in the inductances due to saturation effects, and harmonic content is to use models in which these nonlinearities are stored in several look-up tables [22-24]. Usually, the inductance or the magnetic flux and the torque, each dependent on the machine currents and the rotor position, are stored. This way, results of an FEM model can be implemented and executed in real-time.

The setup in this paper uses the nonlinear model presented in [22-24] for emulating a three-phase, permanent magnet synchronous machine (PMSM) without limiting the capability of emulating machines with an arbitrary number of phases or other machine types. Using any explained real-time model would be also easily possible. The model's electrical part is depicted in Fig. 4. The DUT inverter's output voltages $v_{DUT,x}$ are measured and transformed into the field-oriented, rotating dq-reference frame. The model considers the voltage drops over the constant windings' resistance R_S on the one hand and the variable inductances L_d and L_q in direct and quadrature direction and the flux of the permanent magnet Ψ_{PM} on the other hand, all depending on the motor currents i_d and i_q. These dependencies are stored in three 3-D look-up tables. The discrete elements of the look-up tables are linearized. After transforming them back into the UVW reference frame, the three machine currents serve as reference currents for the device control unit on the machine side.

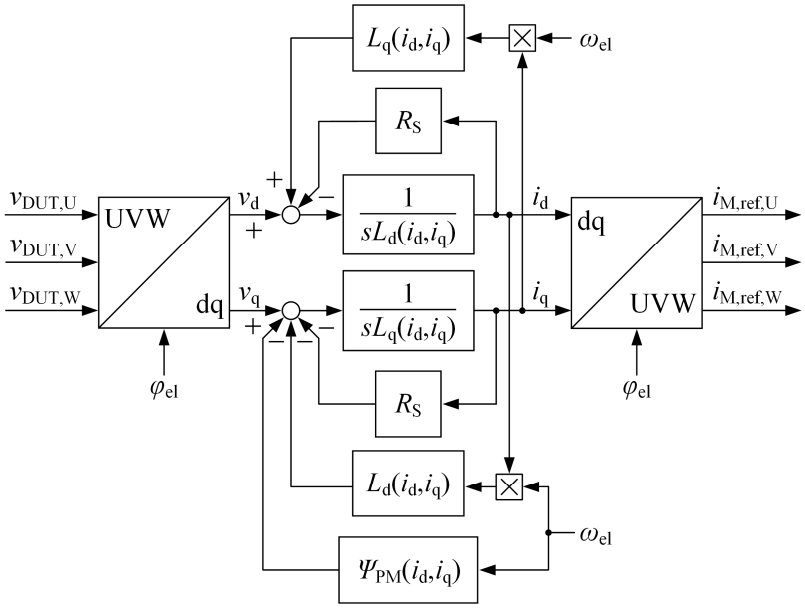

Fig. 4: Block diagram of nonlinear machine model (electrical part)

For the calculation of the inductive voltage drops and the transformation angle, the machine's mechanical behavior is also calculated. The corresponding part of the model is shown in Fig. 5. The electrical circular

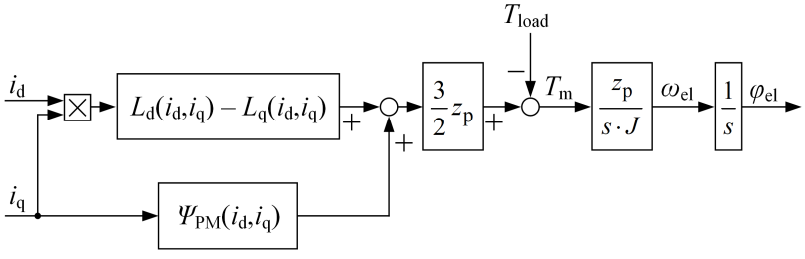

Fig. 5: Block diagram of nonlinear machine model (mechanical part)

frequency ω_{el} and the transformation angle φ_{el} are evaluated by using the machine's number of pole pairs z_p, the drivetrain's inertia J, and if present, an outer load torque T_{load}.

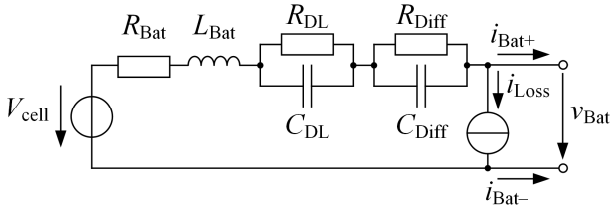

Fig. 6: Circuit diagram of the dynamic battery model

The easiest way to model the battery is as an ideal DC voltage source. The inner resistance and the dynamic behavior of the battery can be considered by simulating additional equivalent resistors and capacitors in series and in parallel to the ideal voltage source [25]. The actual battery current leads to voltage drops over the equivalent elements. Depending on the battery type, its behavior can be simulated more precisely by using more equivalent elements and a look-up table, where the values of the equivalent elements are stored as a function of the state of charge (SOC) and the state of health (SOH) [26]. The implemented equivalent circuit diagram of the used model is shown in Fig. 6. The voltage V_{cell} represents the inner cell voltage that directly depends on the SOC. Furthermore, the equivalent circuit model considers the resistance R_{Bat} and the inductance L_{Bat} of the battery, the dynamic behavior of its diffusion (R_{Diff}, C_{Diff}) and its double layer (R_{DL}, C_{DL}), and additional losses (i_{Loss}).

Device Control Units

The device control units have to calculate switching commands for the dedicated PE modules, so that the actual battery voltage v_{Bat} follows the course of the desired battery voltage $v_{Bat,ref}$, and the actual machine currents $i_{M,x}$ follow the courses of the reference currents $i_{M,ref,x}$. For this purpose, two approaches are possible: a voltage-based one and a current-based one.

In the voltage-based approach, the output voltages of the PE modules are adjusted by an open-loop controller. A multicarrier pulse width modulation (PWM) unit with six equidistant carrier signals evaluates the desired output voltages and determines the corresponding switching commands for the three half bridges per module [27]. Thereby, the average of the module's output voltage over one pulse period follows its desired value.

On the battery side, the reference battery voltage can be realized directly if the coupling inductance is $L_C = 0$ or the current is in the steady state. For the real setup, where dynamic processes are common, a closed-loop voltage control system must be implemented. The control path for that is the resonant circuit consisting of the modules' coupling inductances and the DC link capacitance of the DUT inverter. A state controller is recommended.

On the machine side, currents are used as the reference value. Therefore, the coherence between the control path and the current change must be analyzed in order to calculate the required countervoltages. These countervoltages are adjusted by the PE modules. The ideal control path per phase consists of the coupling inductance L_C. Its voltage equation is

$$v_{Mod} - v_{Mod,out} = L_C \cdot \frac{di_{LC}}{dt} . \tag{2}$$

When referencing to the DUT inverter's output voltages $v_{DUT,x}$ and using the reference currents $i_{M,ref,x}$, the module must supply the following output voltage at the coupling point:

$$v_{Mod,x} = v_{DUT,x} - L_C \cdot \frac{di_{M,ref,x}}{dt} \tag{3}$$

Generally, the control path differs from the ideal coupling inductor and the currents will differ from their reference currents. Hence, an additional current controller is required which can be a proportional controller due to integral behavior of the coupling inductance [8,16].

In this paper, a current-based approach is chosen. Each single module's output current i_{LC} is controlled by the model-predictive controller published in [28]. This establishes a high-bandwidth control strategy and leads to the advantage that every module is an independent current source. Moreover, this offers the option to connect and operate two or any number of modules in parallel in order to increase the overall ampacity. The current controller for each module is implemented on an FPGA, which is located

decentralized on the corresponding PE module. Hereinafter, the realized entity of PE module and decentralized FPGA is called HV module.
The switching commands themselves are determined by a multi-carrier PWM and a contracyclical interrupt, called 'DUT state detection'. Both select one of the seven possible output voltage states. The DUT state detection responds to changes in the DUT output voltages immediately within 500 ns in order to enable a highly dynamic response of the PHIL system.
Four out of seven possible module output voltages ($k = 1$ or $k = 2$ in eq. 1) can be adjusted each by three different switching states. This additional degree of freedom is used to ensure a symmetric current distribution between the three branches per PE module and avoids saturation in the differential-mode chokes. Each of the three possible switching states effects different slew rates and especially directions of change in the courses of the three branch currents i_1, i_2 and i_3, see Table I. In this table, state "1" means that the branch's output potential is connected to the upper DC link potential (and vice versa for state "–1" and the lower DC link potential). State "0" means, that the branch's output potential is connected to the neutral potential φ_0.

Table I: Possible switching states

v_{Mod}	Sw. State	di_1/dt	di_2/dt	di_3/dt
$V_{DC,Sup}/2$	[1 1 1]	0	0	0
$2/6 \cdot V_{DC,Sup}$	[1 1 0]	> 0	> 0	< 0
	[1 0 1]	> 0	< 0	> 0
	[0 1 1]	< 0	> 0	> 0
$1/6 \cdot V_{DC,Sup}$	[1 0 0]	> 0	< 0	< 0
	[0 1 0]	< 0	> 0	< 0
	[0 0 1]	< 0	< 0	> 0
0 V	[0 0 0]	0	0	0
$-1/6 \cdot V_{DC,Sup}$	[–1 0 0]	< 0	> 0	> 0
	[0 –1 0]	> 0	< 0	> 0
	[0 0 –1]	> 0	> 0	< 0
$-2/6 \cdot V_{DC,Sup}$	[–1 –1 0]	< 0	< 0	> 0
	[–1 0 –1]	< 0	> 0	< 0
	[0 –1 –1]	> 0	< 0	< 0
$-V_{DC,Sup}/2$	[–1 –1 –1]	0	0	0

Cyclically, with a higher frequency than the PWM frequency, the device control unit decides by means of the measured values of the branch currents which switching state is most suitable in order to counteract asymmetry. For example, if an output voltage $v_{Mod} = 2/6 \cdot V_{DC,Sup}$ is required and the branch current i_1 is higher than the currents i_2 and i_3, the device control unit selects switching state [0 1 1] in order to decrease current i_1. As soon as i_1 is smaller than i_2 and i_3 and i_2 becomes the highest of these three currents, the switching state changes at the next cyclical interrupt to [1 0 1] without affecting the output voltage.
The PHIL implementation on the machine side is quite simple. The calculated reference currents per phase, each divided through the number of modules connected in parallel if necessary, are sent to the controllers on the HV modules. They adjust very dynamically so that the actual phase currents follow the courses of the reference currents.
In case of battery voltage emulation, the HV modules have to adjust the output voltages. To this end, an output capacitance is required as a controlled system. In some cases, the DUT inverter's DC link capacitance is sufficient, alternatively an additional capacitor must be added between the output terminals of the HV modules emulating the battery. At the same time, an additional voltage control is implemented, which overlays the modules' current controllers. The reduction of control speed, which is caused by an overlain control system, is not a concern because the course of the battery voltage does not include high frequency harmonics.

Implementation in Hardware and Measurement Results

The overall PHIL system is implemented in hardware and can be operated at DC link voltages above $V_{DC,Sup} = 1{,}000$ V. Fig. 7 shows the hardware setup of one HV module. Each HV module is designed to carry currents up to 75 A_{RMS} and reach slew rates up to 5 A/µs. If the device under test (DUT)

requires higher currents or higher slew rates of the current, any number of modules can be operated in parallel to enlarge these characteristic numbers. The HV modules are equipped with a decentralized FPGA performing the current control and the switching state selection part of the device control unit. To avoid a high amount of switching interference, the PWM's carrier frequency is set to f_{PWM} = 200 kHz in this paper. However, variable switching frequencies up to 800 kHz are possible due to the DUT state detection and the switching state selection.

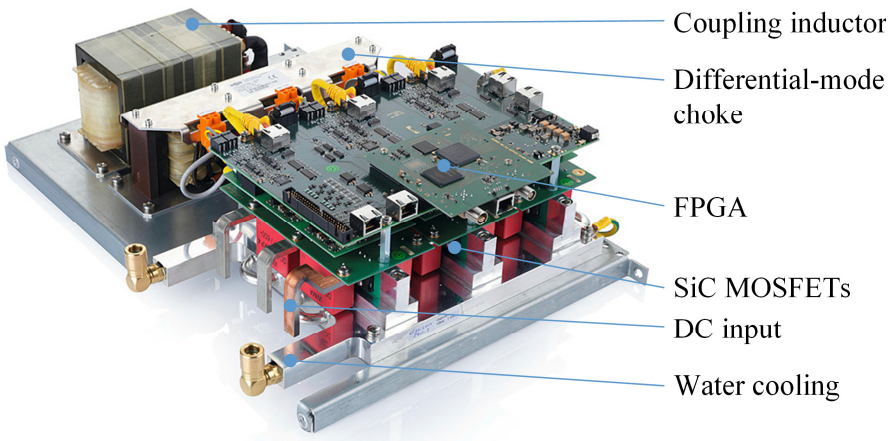

Fig. 7: Setup of the realized HV module

Both the machine and the battery model are implemented on a high-performance real-time FPGA board with very fast I/O interfaces. Only the reference currents are transmitted from this real-time FPGA to the decentralized FPGAs placed on the HV modules. A real-time processor serves as an interface between the real-time FPGA and the control computer. Thereby, model parameters can be changed during run time. The real-time FPGA has a sample time of 8 ns.

For the measurements results in this paper, the setup of Fig. 2 with a single module per battery pole and per machine phase is set up in hardware. The DUT inverter is a three-phase machine inverter. As the focus is on machine currents, the battery voltage is controlled to a constant value. The parameters of the DUT inverter and the PHIL system are summarized in Table II.

The virtual PMSM is adjusted to a constant speed of n = 1,000 rpm. The DUT inverter operates in current control mode. Its reference currents are set to $i_{DUT,ref,d}$ = 0 A in direct direction and $i_{DUT,ref,q}$ = 50 A in quadrature direction. Thus, a nearly constant virtual torque of T_m = 195 Nm occurs. The measurement results of DUT inverter's phase U output current $i_{M,U}$ and its reference value $i_{M,ref,U}$ from the machine model are shown in Fig. 8. The closed-loop control of the DUT inverter leads to a sinusoidal current waveform with an amplitude of 50 A as desired. The real load current follows its reference values from the machine model without any visible deviation. Hence, a detailed view of the currents is observed, see Fig. 9. Due to its high bandwidth, the PHIL system is able to emulate the reference current accurately, even the ripple behavior caused by the DUT inverter's switched-mode operation. Only a small amount of additional current ripple is observed and results the HV modules' own switching behavior. If the PHIL system's DC link voltage is higher than 1,000 V, the magnitude of the additional disturbance ripple content will

Table II: Parameters of the hardware setup

PHIL System Parameters	
DC link voltage $V_{DC,Sup}$	800 V
HV module half bridges' switching frequency	≤ 800 kHz
HV modules per battery pole	1
HV modules per motor phase	1
DUT Inverter Parameters	
Battery voltage v_{Bat} (constant)	500 V
Switching frequency	5.2 kHz
Machine Model Parameters	
Machine type	PMSM
Number of pole pairs z_p	3
Windings resistance R_S	0.01 Ω
Inductance in direct direction L_d	2.7 mH
Inductance in quadrature direction L_q	2.7 mH
Flux of the permanent magnet Ψ_{PM}	0.87 Vs

increase, but the emulation of the desired currents' slew rate is still more accurate than known from other motor emulators.

Conclusion

This paper presents the entire setup of a powerful PHIL system which is suitable for high-voltage and high-frequency application. The setup of an HV module is introduced which behaves as a modular, high-quality current source with a high bandwidth. Each HV module is current-controlled, so multiple modules can be operated in parallel to increase the overall system power. Moreover, two different kinds of control schemes are presented. For the final implementation, the more sophisticated control approach is chosen, which selects the most appropriate switching state in order to counteract an asymmetric current distribution within an HV module. The reference values of the battery and machine currents are calculated by real-time machine and battery models. For this purpose, multiple real-time capable models are introduced. For the machine model in particular, a nonlinear approach using look-up tables is used in the final implementation.
The entire PHIL system is set up in hardware. Its functionality is proven by measurement results, which highlight the strong performance regarding real-time capability and emulation accuracy.

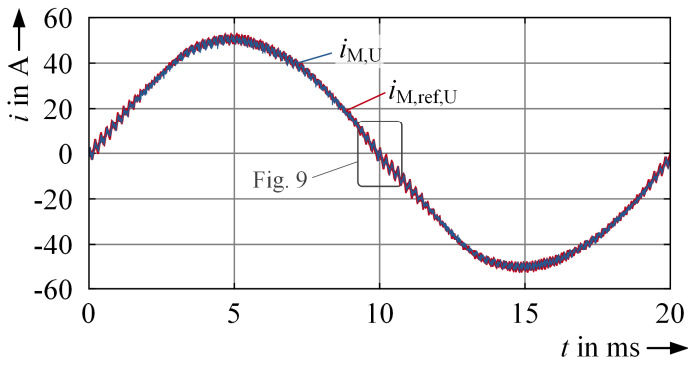

Fig. 8: Measurement of the phase current

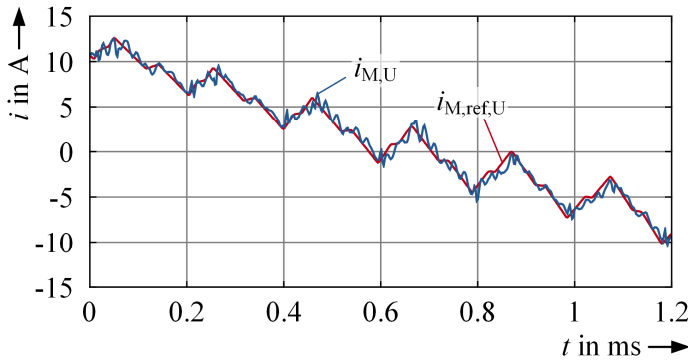

Fig. 9: Detailed view of the measured phase current

References

[1] C. Nemec and J. Roth-Stielow, "Ripple current minimization of an interleaved-switched multi-phase PWM inverter for three-phase machine-emulation," 14th European Conference on Power Electronics and Applications, 2011.

[2] A. Schmitt, J. Richter, M. Braun, and M. Doppelbauer, "Power Hardware-in-the-Loop Emulation of Permanent Magnet Synchronous Machines with Nonlinear Magnetics – Concept & Verification," PCIM Europe, pp. 393-400, 2016.

[3] M. Fischer, S. Petzner, J. Ruthardt, J. Schuster, S. Bintz, and J. Roth-Stielow, "Current Control for a Multiphase Interleaved-Switched Inverter Using Field Oriented Coordinates," 20th European Conference on Power Electronics and Applications, 2018.

[4] A. Schmitt, J. Richter, M. Gommeringer, T. Wersal, and M. Braun, "A Novel 100 kW Power Hardware-in-the-Loop Emulation Test Bench for Permanent Magnet Synchronous Machines with Nonlinear Magnetics," 8th IET International Conference on Power Electronics, Machines and Drives, 2016.

[5] M. Fischer, J. Ruthardt, M. Nitzsche, P. Ziegler, and J. Roth-Stielow, "Investigation on Carrier Signals to Minimize the Overall Current Ripple of an Interleaved-Switched Inverter," PCIM Europe, pp. 1644-1649, 2019.

[6] R. Sudharshan Kaarthik, and P. Pillay, "Emulation of a Permanent Magnet Synchronous Generator in Real-time Using Power Hardware-in- the-loop," International Conference on Power Electronics, Drives and Energy Systems, 2016.

[7] M. Fischer, F. Gliese, J. Ruthardt, M. Zehelein, and J. Roth-Stielow, "Investigation on a Three-Phase Inverter with LC Output Filter for Machine Emulation," 21st European Conference on Power Electronics and Applications, 2019.

[8] M. Fischer, D. Erthle, P. Ziegler, J. Ruthardt, and J. Roth-Stielow, “Comparison of Two Power Electronic Topologies for Power Hardware in the Loop Machine Emulator,” IEEE Applied Power Electronics Conference and Exposition (APEC), pp. 2950-2954, 2020.

[9] S. Lentijo, S. D'Arco, and A. Monti, “Comparing the Dynamic Performances of Power Hardware-in-the-Loop Interfaces,” in IEEE Transactions on Industrial Electronics, vol. 57, no. 4, pp. 1195-1207, 2010.

[10] G. Si and R. Kennel, “Switch mode converter based high performance power-hardware-in-the-loop grid emulator,” 2016 IEEE 2nd Annual Southern Power Electronics Conference (SPEC), pp. 1-6, 2016.

[11] A. Monti, S. D'Arco, and A. Deshmukh, “A new architecture for low cost Power Hardware in the Loop testing of power electronics equipments,” 2008 IEEE International Symposium on Industrial Electronics, Cambridge, pp. 2183-2188, 2008.

[12] S. L. Baciu, S. Trabelsi, B. Amlang, and W. Schumacher, “Linverter a low-harmonic and high-bandwidth inverter based on a parallel multilevel structure,” in 2004 IEEE 35th Annual Power Electronics Specialists Conference, vol. 5, no. 5, pp. 3927–3931, 2004.

[13] M. Fischer, R. Malic, N. Tröster, J. Ruthardt, and J. Roth-Stielow, “Design of a Three-Phase 100 Ampere Linear Amplifier for Power-Hardware-in-the-Loop Machine-Emulation,” IET The Journal of Engineering, no. 17, pp. 4041-4044, 2019.

[14] K. S. Amitkumar, R. Thike, and P. Pillay, “Linear Amplifier-Based Power-Hardware-in-the-Loop Emulation of a Variable Flux Machine,” IEEE Transactions on Industry Applications, vol. 55, no. 5, pp. 4624–4632, 2019.

[15] M. Fischer, J. Ruthardt, V. Ketchedjian, P. Ziegler, M. Nitzsche, and J. Roth-Stielow, “Four-Level Inverter with Variable Voltage Levels for Hardware-in-the-Loop Emulation of Three-Phase Machines,” 22nd European Conference on Power Electronics and Applications, Lyon, France, pp. 1-8, 2020.

[16] M. Fischer, Y. Hu, J. Ruthardt, P. Ziegler, J. Haarer and J. Roth-Stielow, “Comparison of an Interleaved Multi-Branch Inverter and a Four-Level Inverter with Variable Voltage Levels for Emulation of Three-Phase Machines,” 2021 IEEE Energy Conversion Congress and Exposition (ECCE), pp. 2570-2575, 2021.

[17] M. Schnarrenberger, L. Stefanski, C. Rollbühler, D. Bräckle, and M. Braun, “A 50 kW Power Hardware-in-the-Loop Test Bench for Permanent Magnet Synchronous Machines based on a Modular Multilevel Converter,” 20th European Conference on Power Electronics and Applications, 2018.

[18] P. Pillay and R. Krishnan, “Modeling of permanent magnet motor drives,” in IEEE Transactions on Industrial Electronics, vol. 35, no. 4, pp. 537-541, Nov. 1988.

[19] S. Decker, J. Stoss, A. Liske, M. Brodatzki, J. Kolb, and M. Braun, “Online Parameter Identification of Permanent Magnet Synchronous Machines with Nonlinear Magnetics based on the Inverter Induced Current Slopes and the dq-System Equations,” EPE '19 ECCE Europe, 2019.

[20] R. Manju Bhashini and K. Ragavan, “Magnetic Equivalent Circuit for Surface-Mounted PM Motor,” 2018 IEEE International Conference on Power Electronics, Drives and Energy Systems (PEDES), pp. 1-5, 2018.

[21] A. L. Rodríguez, D. J. Gómez, I. Villar, A. López-de-Heredia, and I. Etxeberria-Otadui, “Improved analytical multiphysical modeling of a surface PMSM,” 2014 International Conference on Electrical Machines (ICEM), pp. 1224-1230, 2014.

[22] M. Boesing, M. Niessen, T. Lange, and R. De Doncker, “Modeling spatial harmonics and switching frequencies in PM synchronous machines and their electromagnetic forces,” 2012 XXth International Conference on Electrical Machines, pp. 3001-3007, 2012.

[23] M. Plöger and M. Deter, “Highly precise real-time simulation of E-motors,” in ATZ Elektronik, 2013.

[24] A. Schmitt, J. Richter, U. Jurewitz and M. Braun, “FPGA-Based Real-Time Simulation of Nonlinear Permanent Magnet Synchronous Machines for Power Hardware-in-the-Loop Emulation Systems,” in Industrial Electronics Society, IECON 2014 - 40th Annual Conference of the IEEE, Dallas, 2014.

[25] W. S. Putra, B. R. Dewangga, A. Cahyadi, and O. Wahyunggoro, “Current estimation using Thevenin battery model,” Proceedings of the Joint International Conference on Electric Vehicular Technology and Industrial, Mechanical, Electrical and Chemical Engineering (ICEVT & IMECE), 2015, pp. 5-9.

[26] X. Zhang, W. Zhang, and G. Lei, “A Review of Li-ion Battery Equivalent Circuit Models,” Transactions on Electrical and Electronic Materials, 17, pp. 311-316, 2016.

[27] T. Prathiba and P. Renuga, “Multi Carrier PWM based Multi Level Inverter for High Power Application,” in International Journal of Computer Applications, 2010.

[28] G. Meyer, “Enhanced Power Electronics System for High-Performance Testing of Motor Control Units in a Power HIL Environment,” PCIM Asia 2017; International Exhibition and Conference for Power Electronics, Intelligent Motion, Renewable Energy and Energy Management, pp. 1-8. 2017.